






# New Insights into the Evolution of the Electron Transfer from Cytochrome *f* to Photosystem I in the Green and Red Branches of Photosynthetic Eukaryotes

Carmen Castell <sup>1</sup>, Luis A. Rodríguez-Lumbreras <sup>2</sup>, Manuel Hervás <sup>1</sup>, Juan Fernández-Recio <sup>2</sup> and José A. Navarro <sup>1,\*</sup>

<sup>1</sup>Instituto de Bioquímica Vegetal y Fotosíntesis, CSIC and Universidad de Sevilla, cicCartuja, Sevilla, Spain

<sup>2</sup>Instituto de Ciencias de la Vid y del Vino (ICVV), CSIC—Universidad de La Rioja—Gobierno de La Rioja, Logroño, Spain

\*Corresponding author: Email, jnavarro@ibvf.csic.es; Fax, +34 954 46 01 65.

(Received 10 February 2021; Accepted 15 March 2021)

In cyanobacteria and most green algae of the eukaryotic green lineage, the copper-protein plastocyanin (Pc) alternatively replaces the heme-protein cytochrome *c*<sub>6</sub> (Cc<sub>6</sub>) as the soluble electron carrier from cytochrome *f* (Cf) to photosystem I (PSI). The functional and structural equivalence of 'green' Pc and Cc<sub>6</sub> has been well established, representing an example of convergent evolution of two unrelated proteins. However, plants only produce Pc, despite having evolved from green algae. On the other hand, Cc<sub>6</sub> is the only soluble donor available in most species of the red lineage of photosynthetic organisms, which includes, among others, red algae and diatoms. Interestingly, Pc genes have been identified in oceanic diatoms, probably acquired by horizontal gene transfer from green algae. However, the mechanisms that regulate the expression of a functional Pc in diatoms are still unclear. In the green eukaryotic lineage, the transfer of electrons from Cf to PSI has been characterized in depth. The conclusion is that in the green lineage, this process involves strong electrostatic interactions between partners, which ensure a high affinity and an efficient electron transfer (ET) at the cost of limiting the turnover of the process. In the red lineage, recent kinetic and structural modeling data suggest a different strategy, based on weaker electrostatic interactions between partners, with lower affinity and less efficient ET, but favoring instead the protein exchange and the turnover of the process. Finally, in diatoms the interaction of the acquired green-type Pc with both Cf and PSI may not yet be optimized.

**Keywords:** Cytochrome *c*<sub>6</sub> • Cytochrome *f* • Electron transfer • Photosynthetic green and red lineages • Photosystem I • Plastocyanin.

## Introduction

Oxygenic photosynthesis is a crucial process in the acquisition and storage of solar energy in the biosphere. Globally, it is estimated that photosynthesis captures  $\approx 3 \times 10^{21}$  J year<sup>-1</sup> and is responsible for the annual assimilation of  $\approx 100$  Gt of

carbon (Hall 1976, Field et al. 1998). Photosynthetic productivity is shared roughly equally between terrestrial systems and the oceans, making photosynthesis a global process spread across the entire Earth's surface.

At the molecular level, the productivity of photosynthetic organisms is related to the efficiency of their photosynthetic electron transfer (ET) chain, in which photo-induced electron transport is coupled to the generation of both energy-rich compounds and a proton motive force. The main features of the sophisticated machinery that performs oxygenic photosynthesis are preserved from prokaryotic cyanobacteria to plants. Thus, in the photosynthetic chain, three large membrane complexes coexist: photosystem II (PSII), cytochrome *b*<sub>6</sub>*f* (Cb<sub>6</sub>*f*) and photosystem I (PSI), which are connected by mobile electron transporters (Hervás et al. 2003, Blankenship 2014) (Fig. 1). In plants, ET between the Cb<sub>6</sub>*f* complex and PSI is carried out in the thylakoid lumen of the chloroplast solely by the copper-protein plastocyanin (Pc), whereas the output of electrons from PSI is directed to the iron-sulfur protein ferredoxin (Fd) (Fig. 1A). However, this situation must be taken as an end point in the evolutionary path of the green lineage that, starting from cyanobacteria (considered the ancestors of the eukaryotic chloroplast) and green algae, leads to plants (Fig. 2A) (Falkowski et al. 2004, De la Rosa et al. 2006, Sétif 2006). Conversely, in aquatic systems, photosynthetic microorganisms have maintained alternative redox protein pairs, which can be understood as an adaptation to fluctuations and limitations in the bioavailability of metals in these ecosystems (specifically iron (Fe) and copper (Cu)) (De la Rosa et al. 2006, Moore and Braucher 2008, Nouet et al. 2011, Marchetti et al. 2012). In particular, in most cyanobacteria and unicellular green algae, Pc acts by alternatively replacing the heme-protein cytochrome *c*<sub>6</sub> (Cc<sub>6</sub>) (considered the initial ancestral carrier) when copper is available. Furthermore, the flavoprotein flavodoxin (Fld) replaces Fd under iron-limiting conditions (Hervás et al. 2003, Sancho 2006, Sétif 2006) (Fig. 1A). Thus, plants have lost Cc<sub>6</sub> and Fld as alternative proteins along their evolution within the green lineage, probably due to the particularities of the process

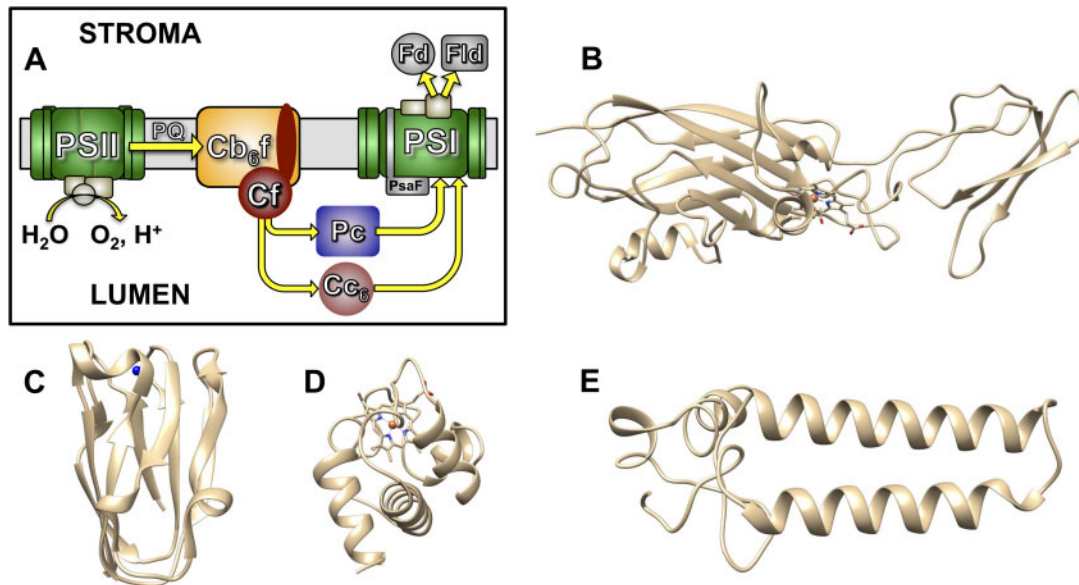


**Fig. 1** (A) Photosynthetic chain and electron transfer pathways (shown by arrows) based on the existence of alternative soluble electron carrier proteins. PQ, plastoquinone; PsaF, PSI subunit involved—in green algae and plants—in the electrostatic interaction with Pc and Cc<sub>6</sub>, the two alternative soluble electron carriers between Cb<sub>6</sub>f and PSI. Backbone representation of photosynthetic proteins of the green alga *Chlamydomonas reinhardtii*: (B) luminal exposed part of Cf in the Cb<sub>6</sub>f complex (Protein Data Bank, PDB code, 1cfm); (C) Pc (PDB code, 2plt); (D) Cc<sub>6</sub> (PDB code, 1cyj); and (E) luminal exposed part of PsaF in PSI (PDB code, 6ijo). The copper (in Pc) and heme (in Cf and Cc<sub>6</sub>) cofactors are highlighted.

of land colonization with respect to the bioavailability of iron and copper (De la Rosa et al. 2006, Pierella Karlusich et al. 2014). The functional and structural equivalences of Pc and Cc<sub>6</sub>, and of Fd and Fld, have been well established (Hervás et al. 1995, Hervás et al. 2003, Hippler and Drepper 2006, Sétif 2006, Pierella Karlusich et al. 2014, Bendall and Howe 2016), and therefore, both couples represent an example of evolutionary functional convergence of unrelated proteins (De la Rosa et al. 2006).

Interestingly, the existence of alternative non-iron proteins is only partially maintained in the red lineage of photosynthetic organisms that diverged from the green lineage along evolution. The red lineage includes, among others, red algae and diatoms (Falkowski et al. 2004) (Fig. 2A). Thus, Fld is present as an alternative to Fd in most algal taxa of the red lineage, including red algae, cryptophytes, stramenopiles (that include diatoms) and haptophytes (Pierella Karlusich et al. 2014). However, Cc<sub>6</sub> is the only soluble donor available in red algae and most algae of the red-plastid lineage, as evidenced by direct protein characterization, genome sequences and transcriptomic analysis of different red algae and stramenopiles, including diatoms (Akazaki et al. 2009, Bowler et al. 2010, Groussman et al. 2015). These works have confirmed a widespread predominance of the *petJ* gene encoding Cc<sub>6</sub> and have validated this protein as the electron carrier from Cb<sub>6</sub>f to PSI in the majority of organisms within the red-plastid lineage (Blaby-Haas and Merchant 2012, Groussman et al. 2015). However, although all the stramenopiles whose genomes have been sequenced have genes for Cc<sub>6</sub>, genome sequencing and metatranscriptomics analysis have also identified *petE* genes, encoding Pc, in several species of oceanic diatoms. This has been explained as gene acquisition from green alga by horizontal gene transfer,

probably as an adaptation to the limitation of iron in their natural habitats (Peers and Price 2006, Marchetti et al. 2012, Groussman et al. 2015, Hippmann et al. 2017). In fact, a particular strain of the open ocean diatom *Thalassiosira oceanica* appears to constitutively replace Cc<sub>6</sub> by Pc, as the two genes that encode Cc<sub>6</sub> in its genome are weakly expressed, presumably reducing its overall need for iron (Peers and Price 2006, Lommer et al. 2012, Kong and Price 2020).

Finally, it is interesting to note that although the Fd/Fld pair has well-conserved common functional characteristics in the vast majority of photosynthetic organisms (Pierella Karlusich et al. 2014), the Cc<sub>6</sub>/Pc pair presents significant variations in different types of organisms, both in the mechanism of interaction with its partners and in their interaction areas (Díaz-Quintana et al. 2008). Although the functional and structural properties of the ‘green’ Cc<sub>6</sub>/Pc pair—and the comparison with equivalent cyanobacterial systems—have been characterized in depth (Hippler and Drepper 2006, Díaz-Quintana et al. 2008, Bendall and Howe 2016), recent works have provided new data on the ET mechanism and protein features in the red-plastid lineage (Bernal-Bayard et al. 2013, Bernal-Bayard et al. 2015, Roncel et al. 2016, Antoshvili et al. 2019, Castell et al. 2021). These data suggest that different strategies have been developed in the evolution of the ET from Cb<sub>6</sub>f to PSI in the green and red branches of eukaryotic photosynthetic organisms.

### Interaction of the Soluble Carriers with PSI

The interaction of Pc and Cc<sub>6</sub> with PSI has been analyzed in vitro and in vivo in several green algae and plants (reviewed in De la Rosa et al. 2006, Hippler and Drepper 2006), and more

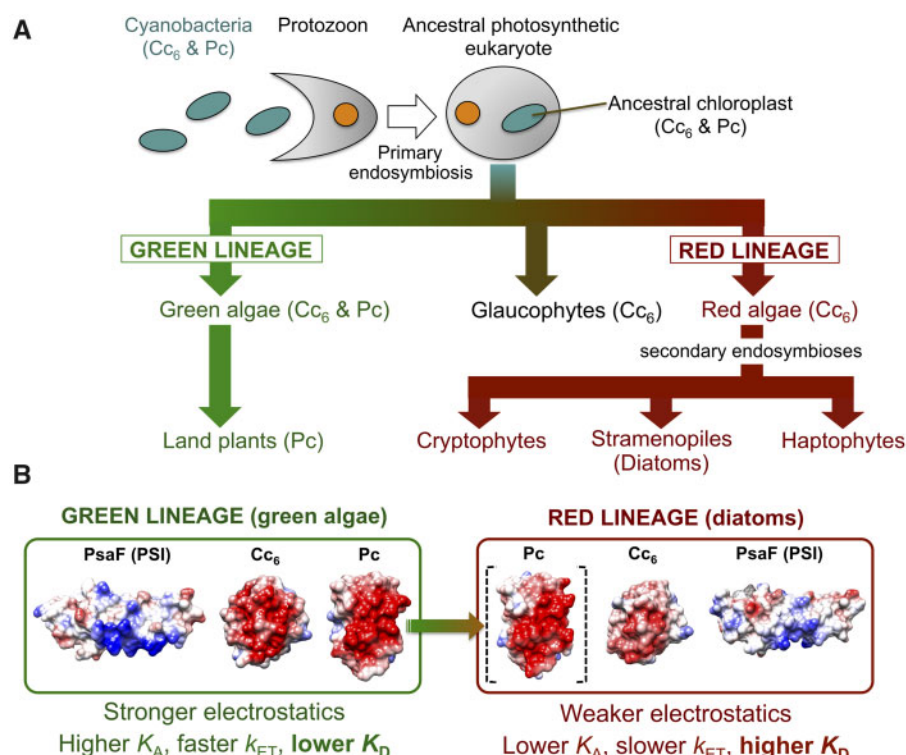


**Fig. 2** (A) Schematic representation of the evolution of the main lineages of photosynthetic eukaryotes and the presence of the electron carriers Pc and Cc<sub>6</sub>. In the green lineage, plants (that only produce Pc) have evolved from green algae, which can produce Pc and Cc<sub>6</sub>. In the red lineage, red algae only produce Cc<sub>6</sub> and are the origin, through secondary endosymbiosis events, of the red-type chloroplast of other secondary algae groups. (B) Electrostatic potential of the charged surface area—involved in the electrostatic interaction with its partners—of Cc<sub>6</sub>, Pc and the PsaF subunit from the green alga *C. reinhardtii*, and of the Cc<sub>6</sub> (PDB code, 3dmi) and modeled PsaF (Bernal-Bayard et al. 2015) from the diatom *P. tricornutum*. The modeled acquired ‘green-type’ Pc of the diatom *T. oceanica* is also shown (in brackets). The proteins are oriented as shown in Fig. 1, with Pc and Cc<sub>6</sub> displaying their electrostatic areas in front and with the hydrophobic patches at the top of both proteins. Electrostatic potential values are shown on a scale from red to blue, corresponding to  $-10.0$  and  $+10.0$  kcal mol<sup>-1</sup>, respectively, at 298 K. K<sub>A</sub> and K<sub>D</sub>, association and dissociation constants, respectively; k<sub>ET</sub>, electron transfer rate constant. See the text for more details.

recently in diatoms (Bernal-Bayard et al. 2013, Bernal-Bayard et al. 2015). In addition to an extensive kinetic characterization of the intermolecular ET processes, structural determinations or models are already available for PSI, Cc<sub>6</sub> and Pc of plants or green algae, as well as for Cc<sub>6</sub> of red algae and diatoms.

### Structural features

Pc is a small (ca. 100 amino acids) protein with a  $\beta$ -barrel tertiary structure that binds a type-1 blue copper cofactor (Fig. 1C). On the other hand, Cc<sub>6</sub> (ca. 90 amino acids) is a typical class I c-type cytochrome with  $\alpha$ -helix-based tertiary structure and a heme group (reviewed in De la Rosa et al. 2006) (Fig. 1D). Because anoxygenic photosynthesis uses cytochromes as electron carriers rather than Pc-like proteins, it is considered that Cc<sub>6</sub> evolved as the ancestral carrier in primitive oxygenic organisms. Both Pc and Cc<sub>6</sub> show a well-defined ET area—determined by the solvent accessibility of the heme group in Cc<sub>6</sub> or the copper ligands in Pc—which is surrounded by a hydrophobic surface patch (Guss and Freeman 1983, Frazão et al. 1995, Inoue et al. 1999, Crowley et al. 2002, Díaz-Moreno et al. 2005; and see Figs. 1C, D, 2B). In addition, Cc<sub>6</sub> and Pc show an electrostatically charged surface area at an equivalent location relative to the ET sites and the hydrophobic patches (Fig. 2B) (De la Rosa

et al. 2006). The electrostatic nature of this patch defines the type of interaction of Pc and Cc<sub>6</sub> with their partners. Thus, in cyanobacteria, the electrostatic patch can be relatively neutral or even positive, but in Pc and Cc<sub>6</sub> of the eukaryotic green lineage, this electrostatic patch always has a strong negative charge (De la Rosa et al. 2006, Hippler and Drepper 2006) (Fig. 2B). One intriguing exception to this general description is fern Pc, in which the acidic region relocates and surrounds the hydrophobic patch, resulting in distinctive electrostatic properties (Kohzuma et al. 1999).

The negative patch of green Cc<sub>6</sub> and Pc has a counterpart in PSI. Biochemical and structural analyses conclude that, in addition to a hydrophobic binding pocket in the PSI core (see below), in green algae and higher plants, there is a strongly positively charged N-terminal region of the PsaF subunit of PSI exposed to the lumen. This N-terminal extension (ca. 70 amino acids; Figs. 1E, 2B) is responsible for the bulk electrostatic interaction between PSI and the negatively charged Pc and Cc<sub>6</sub> donors (Farah et al. 1995, Hippler et al. 1996, Hippler et al. 1998, Sommer et al. 2006).

In the red lineage, the solved crystal structures of Cc<sub>6</sub> from red algae and diatoms show that this soluble carrier maintains the global fold of the ‘green’ Cc<sub>6</sub> (Yamada et al. 2000, Akazaki



et al. 2009). However, with respect to protein surface and functional areas, the Cc<sub>6</sub> of red algae and diatoms still preserves the hydrophobic ET area, but the negative character of the electrostatic area is sensibly reduced (Fig. 2B) (Bernal-Bayard et al. 2013). Interestingly, this decrease in the electrostatic properties of Cc<sub>6</sub> corresponds to equivalent changes in the PSI partner as compared with 'green' systems (Fig. 2B). The recently determined structure of PSI of the red alga *Cyanidioschyzon merolae* (at 4 Å resolution) (Antoshvili et al. 2019) shows both the conservation of the PSI hydrophobic interaction site and the N-terminal region in Psf. However, the luminal Psf extension of this red alga displays a drastic decrease in the number of positive groups, which is also found in other algae of the red lineage, such as diatoms (Fig. 2B). This evidences the existence of significant electrostatic differences in this specific area of PSI between the organisms of the green and red lineages. In conclusion, although the evolution of ET to PSI in red-type organisms has also led to complementary electrostatic interactions between acidic and basic patches in Cc<sub>6</sub> and Psf, respectively, the electrostatic character of both partners is similarly reduced (Bernal-Bayard et al. 2013, Bernal-Bayard et al. 2015) (Fig. 2B).

### The red Pc

A particular case is the existence of *petE* genes, encoding Pc, that have been annotated in the genomes of several strains of oceanic diatom species, as *T. oceanica* and *Fragilariopsis cylindrus*, as well as in the haptophyte *Emiliania huxleyi* and the dinoflagellate *Karenia brevis* (Nosenko et al. 2006, Peers and Price 2006, Blaby-Haas and Merchant 2012). Furthermore, evidence for a functional Pc has been reported in the case of *T. oceanica*, where the holoprotein was detected and partially purified and sequenced (Peers and Price 2006). However, the intracellular levels of Pc reported in *T. oceanica* (3 μM Pc, Peers and Price 2006, Kong and Price 2020) are remarkably low compared to those reported for Pc in cyanobacteria, green algae and plants (Navarro et al. 2011), or to the Cc<sub>6</sub> content described in other diatoms under iron sufficient conditions (Cc<sub>6</sub> ca. 28 μM in the coastal diatom *Phaeodactylum tricornutum*) (Bernal-Bayard et al. 2013, Roncel et al. 2016). On the other hand, the Pc level in *T. oceanica* is comparable to the Cc<sub>6</sub> levels described in *P. tricornutum* under iron-limiting conditions (4–7 μM) (Roncel et al. 2016, Castell et al. 2021). In any case, the Pc-translated region in diatoms is closely related to the Pc from green algae. Consequently, the 'red' acquired Pc actually shows the typical strong negative electrostatics of a 'green-type' Pc (Fig. 2B; and see below) (Castell et al. 2021).

The expression of a functional Pc in diatoms raises, however, two questions that remain to be clarified. First, it requires a specific copper-transporting system to the thylakoid that has not yet been found. High-affinity copper uptake systems have been described in *T. oceanica* (Kong and Price 2019), but a specific thylakoid transport system is also expected to include at least a P-type ATPase transporter located in the thylakoid membrane, which delivers Cu to the lumen to be incorporated into Pc (Guo et al. 2010, Guo et al. 2015, Nouet et al. 2011, Blaby-Haas and Merchant 2012, Kong and Price 2019). This is an

important point since, in the absence of specific mechanisms of copper import into the thylakoid lumen, the copper available to be incorporated into Pc would probably be limited (Ho et al. 2003, Levy et al. 2008, Twining and Baines 2013, Castell et al. 2021). The second question lies in the regulatory mechanism by which a putative Pc could act as an alternative to Cc<sub>6</sub> in diatoms. In cyanobacteria and green algae, copper levels radically determine the expression of one or another protein through precisely regulated mechanisms, including transcription regulators, metal sensors and proteases that have not been found in diatoms (Merchant et al. 2020, García-Cañas et al. 2021). In addition, it has been reported in diatoms that not only low levels of copper but also sufficient levels of iron induce a drastic reduction in Pc transcripts, which, on the contrary, increase under iron-limiting conditions (Lommer et al. 2012, Marchetti et al. 2012, Hippmann et al. 2017, Rizkallah et al. 2020). Recently, a moderate 3-fold decrease in the Pc content (from 3 to 1 μM) has been reported in *T. oceanica* under copper deficiency (Kong and Price 2020). On the other hand, Cc<sub>6</sub> levels in diatoms seem to depend mainly on the availability of iron (Roncel et al. 2016, Castell et al. 2021).

### Kinetic analysis

In addition to the knowledge of the electrostatic properties of green-type Pc, Cc<sub>6</sub> and psf, a large set of fast time-resolved kinetic data on PSI reduction is available. All these data indicate that the long-range electrostatic attraction between strongly charged complementary patches—acidic in Pc and Cc<sub>6</sub> and basic in Psf—drives the formation of an initial transient complex in green algae and plants. Further short-range hydrophobic interactions would also be involved in the reorganization of the complex and its fine tuning, to reach an effective configuration leading to an efficient ET (Hippler et al. 1996, Hippler et al. 1998, Sommer et al. 2006). In fact, the structural properties of PSI and the electron donors in the green lineage ensure both efficient partner association ( $K_A$  up to  $\approx 10^5 \text{ M}^{-1}$ ) and ET rates ( $k_{ET}$  up to  $\approx 10^5 \text{ s}^{-1}$ ) (Bottin and Mathis 1985, Haehnel et al. 1994, Hervás et al. 1995, Drepper et al. 1996, Sigfridsson et al. 1996, Hippler et al. 1998, Molina-Heredia et al. 2003, Klughammer and Schreiber 2016). Again, the exception to this general description is fern Pc: its distinctive electrostatic properties still allow this protein to interact with PSI but with a lower affinity ( $K_A \approx 10^4 \text{ M}^{-1}$ ) and ET rate ( $k_{ET} \approx 10^3 \text{ s}^{-1}$ ) (Navarro et al. 2004).

The high efficiency of the green lineage in the formation of the [donor:PSI] complex and in the ET step has, however, a derived disadvantage. Obviously, PSI reduction must be followed by the dissociation of the reactants, but the too strong electrostatic interaction in the green complexes implies a limitation to this dissociation and, therefore, for a new subsequent redox cycle (Finazzi et al. 2005, Kuhlert et al. 2012). In fact, the release of oxidized Pc (and probably Cc<sub>6</sub>) from PSI represents the kinetic limiting step in the ET from Cb<sub>6</sub>f to PSI in eukaryotic 'green' organisms (Drepper et al. 1996, Finazzi et al. 2005).

In the red lineage, the kinetic analysis of PSI reduction by Cc<sub>6</sub> in the diatom *P. tricornutum* indicated the occurrence of a mechanism similar to that previously described in the green lineage systems. Thus, ET takes place according to

an initial protein–protein encounter complex, followed by a reorganization process leading to an optimized final configuration (Bernal-Bayard et al. 2013). However, the kinetic data make evident the weaker electrostatic nature of the interaction, in agreement with the also weaker surface charges of both Cc<sub>6</sub> and PsaF. Consequently, and in comparison with the green-type systems, the red-type system of *P. tricornutum* showed lower values both for the binding affinity of Cc<sub>6</sub> to PSI ( $K_A \approx 7 \times 10^3 \text{ M}^{-1}$ ) and ET ( $k_{ET} \approx 2 \times 10^4 \text{ s}^{-1}$ ), in addition to a lower efficiency in the formation of the properly arranged [Cc<sub>6</sub>:PSI] complex (Bernal-Bayard et al. 2013), all of which intriguingly reminds the case of the fern [Pc:PSI] system. In this respect, ET kinetics determined by Dual-KLAS/NIR in the cyanobacterium *Synechocystis* sp. PCC 6803 (with a Pc also having decreased electrostatic properties) showed a much tighter coupling of the redox state of Pc to PSI that can be explained as a higher complex turnover (Theune et al. 2021). Interestingly, an in vitro kinetic analysis showed that the interaction of *P. tricornutum* PSI with green algae Cc<sub>6</sub> is more efficient kinetically than the native diatom system, with three times and two times higher  $K_A$  and  $k_{ET}$  values, respectively (Bernal-Bayard et al. 2013). This suggests that the native diatom Cc<sub>6</sub>/PSI couple (and maybe the fern complex) represents a compromise between a lower efficiency in ET and a facilitated turnover, due to a lower binding affinity. Finally, there are no functional data available for the interaction of red PSI with the native ‘green-type’ acquired Pc (as in *T. oceanica*). However, kinetic data indicated that *P. tricornutum* PSI is able to react with the acidic Pc of green algae and plants, although it does much less efficiently than with *P. tricornutum* Cc<sub>6</sub> ( $k_{ET} \approx 3 \times 10^2 \text{ s}^{-1}$  vs.  $2.2 \times 10^4 \text{ s}^{-1}$ , respectively), demonstrating the formation of less-optimal functional complexes (Bernal-Bayard et al. 2013, Bernal-Bayard et al. 2015). However, this efficiency was even doubled in Pc mutants of *Chlamydomonas reinhardtii* (green alga) in which negative charges were replaced for positive ones, trying to mimic the electrostatics of diatom Cc<sub>6</sub> (Bernal-Bayard et al. 2015). Therefore, while an alternative Pc in diatoms could represent a favorable adaptation to iron limitation, its ‘green-type’ character may limit its ET efficiency (Bernal-Bayard et al. 2015, Antoshvili et al. 2019). Even so, a recent work (Castell et al. 2021) has shown that the heterologous expression in *P. tricornutum* of the *C. reinhardtii* Pc mutant more effective in reducing diatom PSI (Pc E85K; Bernal-Bayard et al. 2015) seems to promote an increased growth under iron-limiting conditions, and so to act as a functional alternative to native Cc<sub>6</sub> (Castell et al. 2021).

### 3D structural data on the complexes

Until very recently there were not solved 3D structures at atomic resolution for intermolecular complexes of PSI with the electron donors Pc or Cc<sub>6</sub>. However, from kinetic data, mutagenesis studies, mass spectrometry analysis and computational modeling, it has been possible to propose structural models for the binding of the two soluble electron donors to PSI in green organisms. These models show that this interaction comprises both a global electrostatic attraction and short-range hydrophobic contacts (Hippler et al. 1996, Sommer et al.

2004, Sommer et al. 2006). The latter involve the hydrophobic patches of Pc/Cc<sub>6</sub> and the luminal i/j loops of the PsaA/B subunits in PSI, including the PsaA W651/PsaB W627 residues near P700 (photosystem I primary donor) as part of the ET pathway (Sommer et al. 2004, Busch and Hippler 2011). Electrostatic interactions mainly involve complementary charges in the Pc/Cc<sub>6</sub> negative areas and common positive groups in the PsaF subunit but also include negative groups in PsaB that are required to favor the unbinding of the oxidized donor from PSI (Sommer et al. 2006, Busch and Hippler 2011).

The main features of the interaction between green PSI and Pc have been recently corroborated in the high-resolution structure of a triple complex of plant PSI with Fd and Pc, solved by cryo-electron microscopy (Caspy et al. 2020). The analysis of the PSI–Pc binding confirms that the association of Pc depends principally on hydrophobic interactions, mainly—but not only—around the two tryptophan residues of PSI near P700, with the two copper-ligand His residues in Pc located adjacent to these tryptophan groups. In addition, stabilization of Pc binding occurs mostly through interactions between the positive patch in PsaF and negatively charged Pc residues (D42, D44, E43 and E45), although there are also other additional—but weaker—interactions of PsaF with other negative groups in Pc (Caspy et al. 2020).

In the red lineage, the structure of the [Cc<sub>6</sub>:PSI] transient ET complex of the diatom *P. tricornutum* has been analyzed by computational docking and compared to the equivalent model complex in the green lineage (Fig. 3) (Bernal-Bayard et al. 2015). The *P. tricornutum* model nicely explains why the Cc<sub>6</sub>/PSI redox couple shows a lower efficiency in diatoms compared to green systems, regarding both the formation of the ET complex and the ET reaction. Thus, in the most energetically favorable docking orientations of the diatom [Cc<sub>6</sub>:PSI] complex, the two tryptophan residues of PSI (PsaA W652/PsaB W624), equivalent to those forming the hydrophobic binding site and the ET path to P700 in green organisms, were located at a relatively long

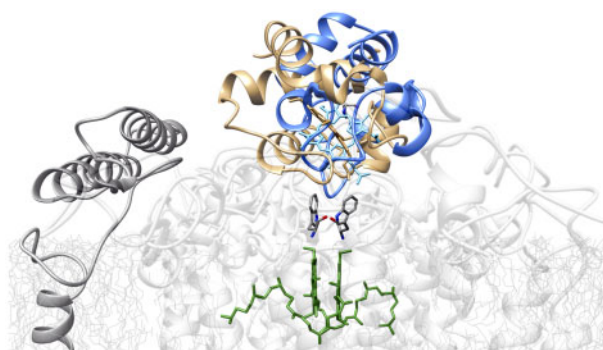


Fig. 3 Best-energy docking models for efficient ET (PsaA W652/PsaB W624 and Cc<sub>6</sub> heme groups at <3.0 Å distance) between *P. tricornutum* PSI and *P. tricornutum* or *M. braunii* Cc<sub>6</sub>. Membrane lipids and PsaA/B subunits of PSI (in light grey), the PsaF subunit of PSI (in dark grey), P700 (in green) and Cc<sub>6</sub> of *P. tricornutum* (in blue) or *M. braunii* (in light brown) are depicted. PSI W652/W624 groups, located in the ET pathway between P700 and the cytochromes, are also shown. PSI:Cc<sub>6</sub> models correspond to the coordinates described in Bernal-Bayard et al. (2015).

distance ( $\approx 10\text{--}20\text{ \AA}$ ) from the  $\text{Cc}_6$  heme. On the contrary, the [ $\text{Cc}_6$ :PSI] docking models that seemed to have the most efficient orientations for ET (PsaA W652/PsaB W624 within  $3.0\text{ \AA}$  distance from the  $\text{Cc}_6$  heme) did not show electrostatic interactions involving the PsaF positive patch or any other relevant favorable interactions (Fig. 3, and see below) (Bernal-Bayard et al. 2015). Altogether, this suggests that the most efficient ET orientations in the *P. tricornutum* [ $\text{Cc}_6$ :PSI] complex are not energetically optimized (Bernal-Bayard et al. 2015). Interestingly, it has been recently reported in the red algae *C. merolae* that the reduction in isolated PSI by a cyanobacterial  $\text{Cc}_6$  was not affected by the removal of the PsaF subunit (Antoshvili et al. 2019). Therefore, it is possible that in the red lineage the PsaF subunit may have a minor role in the interaction with the  $\text{Cc}_6$  donor compared to the green lineage. It should be noted that the low-energy docking orientations between the PSI of *P. tricornutum* and the  $\text{Cc}_6$  of the green alga *Monoraphidium braunii*, placed the two tryptophans of PSI and the  $\text{Cc}_6$  heme at shorter distances, in accordance with the more efficient kinetic data of their cross-reaction (Bernal-Bayard et al. 2013, Bernal-Bayard et al. 2015).

The docking model of the *P. tricornutum* [ $\text{Cc}_6$ :PSI] complex (Fig. 3) shows a different orientation with respect to the complex previously described in the *C. reinhardtii* green system (Hippler et al. 1996, Sommer et al. 2004, Sommer et al. 2006, Busch and Hippler 2011). In the latter, there are specific interactions involving the negative patch of  $\text{Cc}_6$  and positive residues of PsaF, as well as a strong salt bridge between the adjacent R66 and D65 groups in  $\text{Cc}_6$  and the R623/D624 pair of PsaB in PSI, which results in a distance between redox cofactors of  $\approx 14\text{ \AA}$  (Sommer et al. 2006, Busch and Hippler 2011). However, the D65 group is not conserved in *P. tricornutum*, and thus, it cannot stabilize this orientation, resulting in a less favorable overall binding energy. Interestingly, the docking model of the complex between *M. braunii*  $\text{Cc}_6$  and *P. tricornutum* PSI shows strong interactions between the negative patch of  $\text{Cc}_6$  and positive residues of PsaF, as described in the equivalent native complex of *C. reinhardtii* (Fig. 3) (Sommer et al. 2006).

Finally, in diatoms a 3D structure of the interaction of the native 'green-type' acquired Pc and PSI is not available. However, docking simulations performed for the interaction between *P. tricornutum* PSI and *C. reinhardtii* Pc (Bernal-Bayard et al. 2015) showed that the best-energy model for an efficient docking displays a strong electrostatic interaction between the PsaF positive patch and Pc negative residues (D42, E43 and D44), which are equivalent to those described in the Pc/PSI complex of plants (Bernal-Bayard et al. 2015, Caspy et al. 2020). In agreement with this model, it was recently reported that the reduction reaction of PSI of the red alga *C. merolae* by a plant Pc was strongly inhibited when depleting the PsaF subunit (Antoshvili et al. 2019).

## Interaction of $\text{Cb}_6\text{f}$ with the Soluble Carriers

### Structural and kinetic analyses

After their oxidation by PSI, Pc and  $\text{Cc}_6$  have to be reduced again by cytochrome *f* (Cf), a subunit of the  $\text{Cb}_6\text{f}$  complex and

the exit point of electrons to the luminal soluble electron acceptors (Cramer 2019). Cf (a *c*-type cytochrome with ca. 290 amino acids) have been structurally characterized in cyanobacteria and organisms of the green lineage, both as the entire protein within the  $\text{Cb}_6\text{f}$  complex and as a soluble truncated form (Martinez et al. 1994, Chi et al. 2000, Kurisu et al. 2003, Stroebel et al. 2003). Unique features of Cf include the N-terminal tyrosine Y1 as an unusual heme-binding residue (Martinez et al. 1994, Chi et al. 2000). Moreover, the overall protein fold is also unusual for a *c*-type cytochrome, as it displays a large and elongated hydrophilic domain (ca. 250 amino acids) with a  $\beta$ -barrel-based structure, exposed to the thylakoid lumen (Kurisu et al. 2003, Stroebel et al. 2003). This hydrophilic domain is anchored to the membrane by a single transmembrane  $\alpha$ -helix (Fig. 1B). In addition, the lumen-exposed region exhibits a large and a small, flat domain, connected by a bend, with the larger domain containing the heme group and the Y1 ligand, which are solvent exposed (Martinez et al. 1994) (Figs. 1B, 4). The green-type Cf shows a positively charged surface patch at the interface of the large and small domains, complementary to the negative region of Pc or  $\text{Cc}_6$  (Martinez et al. 1994, Soriano et al. 1997) (Fig. 4). As will be discussed later, in organisms from the green lineage both the large and the small domain are involved in the docking of Pc or  $\text{Cc}_6$ .

Regarding the red lineage, the surface electrostatic potential computed on structural models of *P. tricornutum* and *T. oceanica* Cf (Fig. 4) shows the conservation of the ET exposed area around the Y1 and the heme, as well as a positive area placed in an equivalent position relative to the green-type Cf (Fig. 4). However, due to the substitution of positive groups in the interface of the large and small domains, in the red lineage the positive electrostatic potential of this area in the Cf surface is sensibly reduced (Fig. 4). Therefore, similar and parallel changes occur in Cf and psaF, also in accordance with the decreased electrostatic character of  $\text{Cc}_6$ . However, in the case of *T. oceanica* Cf, it is interesting to note the presence of positive groups outside the usual ET region around the heme-exposed area (Fig. 4).

Kinetic data for native proteins are only available for the Pc/Cf interaction (reviewed in Bendall and Howe 2016), since the overlap between the absorbance spectra of  $\text{Cc}_6$  and Cf prevents to accurately follow the kinetics of the ET reaction between both native cytochromes (Grove and Kostic 2003). In eukaryotes, the Pc/Cf interaction has been studied in green algae and plants (Qin and Kostic 1993, Meyer et al. 1993, Kannt et al. 1996, Soriano et al. 1997, Gong et al. 2000, Schlarb-Ridley et al. 2003). The final conclusion, obtained not only from kinetic data but also from computational and structural NMR studies (see below), is that ET from Cf to Pc occurs following a similar mechanism (binding, reorganization and ET) to that described for PSI reduction (Cruz-Gallardo et al. 2012, Schilder and Ubbink 2013). Again, this mechanism involves long-range electrostatic attraction for initial binding and preorientation of the two partners, as well as short-range hydrophobic contacts to achieve a productive configuration for ET. Given that previous structural and functional data have established the general functional equivalence of Pc and  $\text{Cc}_6$  (De la Rosa et al. 2006,



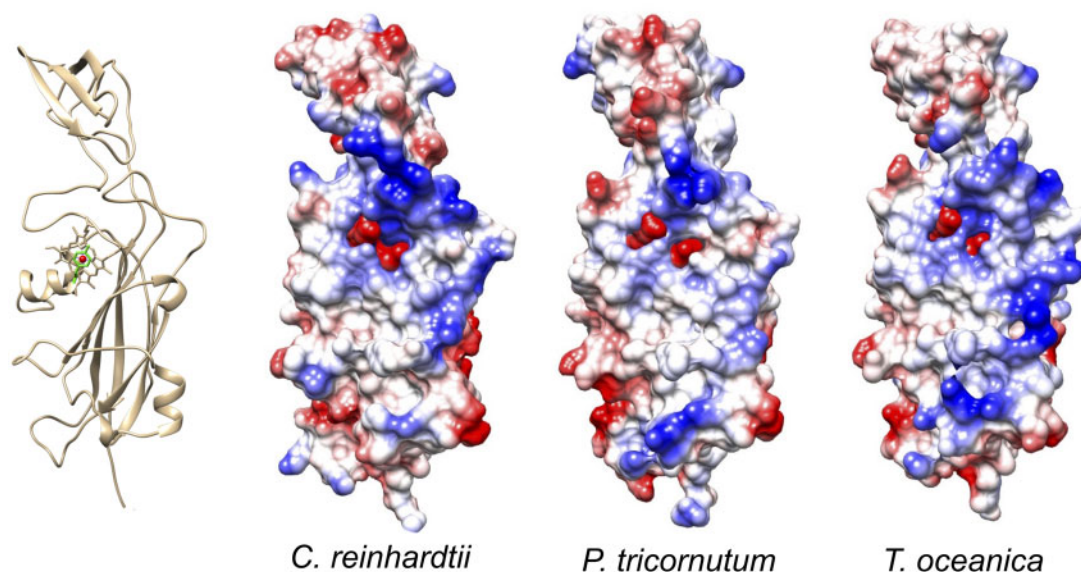


**Fig. 4** (Left) Backbone representation of the exposed luminal domain of Cf of the green alga *C. reinhardtii*. The view displays in front both the heme group and the bound Tyr1 (in green). (Right) Surface electrostatic potential distributions of *C. reinhardtii* Cf and the structural models of *P. tricornutum* and *T. oceanica* Cf. The proteins are oriented as shown in the backbone representation on the left, and electrostatic potential values are shown on the same scale as in **Fig. 2**. See the text and **Supplementary Appendix S1** for more details.

Hippler and Drepper 2006), the hypothesis that a similar mechanism controls the ET reaction of Cf with  $Cc_6$  in green-type organisms seems reasonable.

### Structure of the complexes in the green lineage

Several NMR-based structures of plant [Cf:Pc] complexes have been described (Ubbink et al. 1998, Lange et al. 2005) (**Fig. 5A**). In addition, Brownian Dynamics (BD) simulations have studied the Cf interaction with the soluble electron acceptors in plants and in the green alga *C. reinhardtii* (Gross and Pearson 2003, Musiani et al. 2005, Haddadian and Gross 2006, Fedorov et al. 2019). However, these types of studies have been absent until now in organisms of the red lineage.

The NMR-based structure of the plant [Cf:Pc] complex (**Fig. 5A**) shows a relatively large complex interface, involving both the large and small domains of Cf, forming the so-called 'side-on' relative orientation (in contraposition to the 'head-on' orientation that appears in some complexes of cyanobacteria) (Ubbink et al. 1998, Cruz-Gallardo et al. 2012). As expected, the complex shows electrostatic interactions between positively charged residues in Cf and negatively charged groups in Pc, as well as interactions between both hydrophobic patches, thus providing an efficient ET pathway (Fe–Cu distance of 10.9 Å) (Ubbink et al. 1998) (**Fig. 5A**).

Although a detailed analysis on NMR-based docking models of the [Cf:Cc<sub>6</sub>] complex has been carried out in the cyanobacterium *Nostoc* (Díaz-Moreno et al. 2014), in eukaryotic organisms, the available data are limited to BD simulations applied to the green [Cf:Cc<sub>6</sub>] (and [Cf:Pc]) complex of *C. reinhardtii* (Gross and Pearson 2003, Haddadian and Gross 2005, Haddadian and Gross 2006; and see below). These studies demonstrated the functional equivalence of the hydrophobic and electrostatic areas in both green Pc and Cc<sub>6</sub>. As described previously for

the Cf:Pc interaction, hydrophobic residues around the heme of Cf (including Y1) interact with hydrophobic residues surrounding the Cc<sub>6</sub> heme. On the other hand, electrostatic attractive interactions involve positive groups in Cf—located in both the large and small domains—and negative groups in Cc<sub>6</sub>. This results in a 'side-on' orientation, which also shows a relatively large interface (Haddadian and Gross 2005; and see **Fig. 5B**). In conclusion, the comparison of the green [Cf:Pc] and [Cf:Cc<sub>6</sub>] complexes confirms the key role of the electrostatic and hydrophobic areas in protein binding and, therefore, in achieving an efficient ET, but also the role of the small Cf domain in stabilizing the proper docking orientations of Pc and Cc<sub>6</sub>.

### Structural modeling of the complexes in the red lineage

As mentioned above, there are no structural data available about the [Cf:Cc<sub>6</sub>] (and [Cf:Pc]) complexes in organisms of the red lineage. However, ET proteins, and in particular, *c*-type cytochromes, have been shown to be structurally quite rigid, and thus, BD and docking approaches treating Cf and Cc<sub>6</sub> as rigid bodies have been widely used (Haddadian and Gross 2005, Haddadian and Gross 2006, Cruz-Gallardo et al. 2012, Bernal-Bayard et al. 2015). Here, we have carried out docking simulations to study the [Cf:Cc<sub>6</sub>] complex in the red lineage by using pyDock, a protein–protein rigid-body docking protocol that uses electrostatics and desolvation energy to score the generated docking poses (Jiménez-García et al. 2013; and see **Supplementary Appendix S1**). To validate our analysis, the same approach has also been used to explore the [Cf:Cc<sub>6</sub>] complex of the green alga *C. reinhardtii*, previously studied by BD simulations (Gross and Pearson 2003, Haddadian and Gross 2005, Haddadian and Gross 2006). Our results indicate that

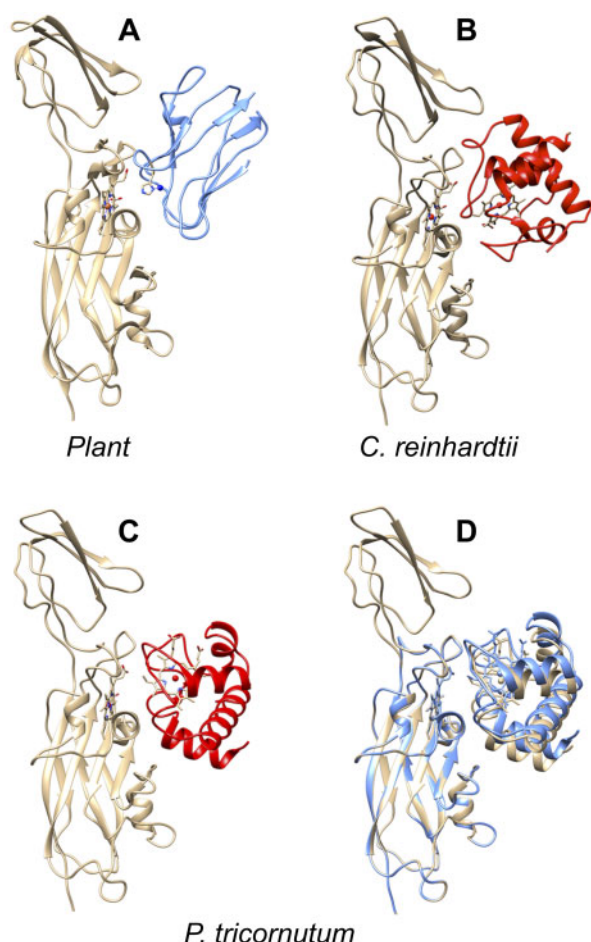


**Fig. 5** (A) Representative structure for the plant Cf:Pc complex (turnip Cf and spinach Pc; obtained from PDB code 2pcf) (Ubbink et al. 1998). Pc is colored in blue and the copper-bound His87 is shown. Best-energy docking models for efficient ET between Cf and Cc<sub>6</sub> (in red) of (B) the green alga *C. reinhardtii* (rank 1, docking energy  $-32.0$  a.u., distance between Fe in Cf to heme in Cc<sub>6</sub> of  $8.2$  Å) and (C) the diatom *P. tricornutum* (rank 6, docking energy  $-24.7$  a.u., distance between Fe in Cf to heme in Cc<sub>6</sub> of  $8.0$  Å, the shortest distance model). (D) Superimposed docking models of the *P. tricornutum* [Cf:Cc<sub>6</sub>] complex (in C) and the model (in blue) corresponding to a truncated Cf without the small domain (rank 2, docking energy  $-31.0$  a.u., distance between Fe in Cf to heme in Cc<sub>6</sub> of  $8.4$  Å). See **Supplementary Appendix S1** for more details.

the best-energy docking models for the *C. reinhardtii* complex converge toward an orientation with the shortest cofactors distance (**Fig. 5B**). This orientation is basically identical to the models previously described (Haddadian and Gross 2005, Haddadian and Gross 2006).

In the case of *P. tricornutum*, the energy-distance landscape of the docking models of the native [Cf:Cc<sub>6</sub>] complex also shows that the lowest-energy models converge toward orientations with a short distance between the heme iron in Cf and the heme group in Cc<sub>6</sub> (**Supplementary Fig. S1**). As it was the case in the [Cc<sub>6</sub>:PSI] complex (Bernal-Bayard et al. 2015; and see above), the *P. tricornutum* [Cf:Cc<sub>6</sub>] docking complex has a different orientation compared with the previously described model of the equivalent green complex in *C. reinhardtii*

(Haddadian and Gross 2005) (**Fig. 5B, C**). Thus, the docking models of the *P. tricornutum* [Cf:Cc<sub>6</sub>] complex with the lowest—most favorable—energies and optimal distances between the Fe in Cf and the heme cofactor in Cc<sub>6</sub> (energies from  $-25$  to  $-22$  a.u.; distances between  $8$  and  $10$  Å) have a ‘head-on’ orientation (**Fig. 5C**), more similar to that described previously in cyanobacterial systems. These orientations display smaller interfaces and weaker electrostatic interactions, with hydrophobic interactions being more relevant (Crowley et al. 2001, Cruz-Gallardo et al. 2012) (**Fig. 5C**). In the ‘side-on’ configuration observed in the complex of *C. reinhardtii*, negatively charged residues of Cc<sub>6</sub> (D2, E54, K57, D65, R66, E70 and E71) have significant contacts with positive residues in Cf, in particular with the K65, K188 and K189 groups. However, in *P. tricornutum*, the E54 and D65 groups in Cc<sub>6</sub> and K189 in Cf are not conserved and cannot stabilize this ‘side-on’ orientation. On the contrary, the orientation in *P. tricornutum* involves relevant electrostatic interactions between E28 in Cc<sub>6</sub> and residues K65 and K187 in Cf, as well as between residues R66 and K57 in Cc<sub>6</sub> and residues E108 and E164 in Cf. As a consequence, the small domain of *P. tricornutum* Cf appears to have only a minor role in the interaction with Cc<sub>6</sub> (**Fig. 5C**). In fact, the simulated deletion of the Cf small domain did not significantly affect the docking to Cc<sub>6</sub> (**Fig. 5D**). This latter result is in contrast with the docking simulation in *C. reinhardtii*, in which the deletion of the Cf small domain affected the binding positions on Cf of both Pc and Cc<sub>6</sub> (Haddadian and Gross 2006). Interestingly, ‘side-on’ docking orientations can be found in *P. tricornutum* that are relatively similar to the best-energy models obtained in *C. reinhardtii*. However, although these orientations have short distances between the Fe in Cf and the heme cofactor in Cc<sub>6</sub> (between  $9.0$  and  $10.5$  Å), they have unfavorable higher energies (from  $-15$  to  $-9$  a.u.) (**Supplementary Fig. S1**).

Finally, it is interesting to analyze the modeled [Cf:Pc] complex of *T. oceanica* in comparison with the above-described [Cf:Cc<sub>6</sub>] complex of *P. tricornutum*, as well as with the equivalent [Cf:Pc] complex of the green lineage. Remarkably, the docking between *T. oceanica* Cf and Pc produced a much larger population of low-energy docking orientations than the *P. tricornutum* [Cf:Cc<sub>6</sub>] complex. This indicates higher binding affinities, possibly as a result of the stronger electrostatics of the acquired ‘green-type’ Pc (**Fig. 2B, Supplementary Fig. S1**). However, in *T. oceanica*, the energy-distance landscape does not converge toward a single prevalent low-energy orientation with a short distance between Cu (in Pc) and Fe (in the Cf heme). On the contrary, it results in a series of different orientations in a similar range of energies and distances (**Fig. 6A–C, Supplementary Fig. S1**). This suggests that the Cf:Pc interaction in *T. oceanica* is not optimized in a single group of solutions with a favorable combination of interactions and distances for ET. Therefore, different protein–protein orientations might be functionally possible and could coexist. The best-energy/distance balanced dockings of the *T. oceanica* Cf:Pc modeled complex include: (i) a ‘head-on’ configuration, similar to some cyanobacterial complexes, involving the hydrophobic patches of both Cf and Pc with no interactions between the electrostatic areas or the Cf small domain (energy of  $-24.2$  a.u. and the shortest Fe–Cu distance



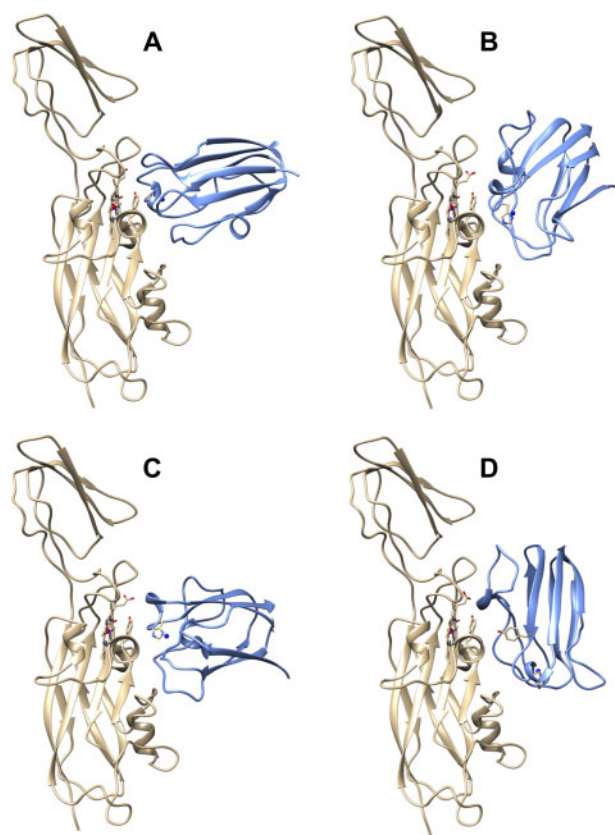


**Fig. 6** (A–C) Representative best-energy docking models for efficient ET between the modeled Cf and Pc (in blue) of the diatom *T. oceanica* (selected by the shorter distances between Fe in Cf and Cu in Pc). The Cf heme, the iron-bound Tyr1 and the copper-bound His88 in Pc are shown. (A) Rank 62, docking energy  $-24.2$  a.u., distance between Fe in Cf to Cu in Pc of  $11.1$  Å (the shortest distance model). (B) Rank 8, docking energy  $-31.1$  a.u., distance between Fe in Cf to Cu in Pc of  $12.7$  Å. (C) Rank 16, docking energy  $-30.1$  a.u., distance between Fe in Cf to Cu in Pc of  $12.2$  Å. (D) Best-energy docking model showing the Tyr84 group in Pc (rank 1, docking energy  $-38.4$  a.u., distance between Fe in Cf to Cu in Pc of  $20.5$  Å). See the text and [Supplementary Appendix S1](#) for more details.

of  $11.1$  Å (**Fig. 6A**); (ii) a ‘side-on’ configuration, more similar to the green complexes (**Figs. 5A, 6B**), involving the electrostatic and hydrophobic patches of both proteins and the small domain of Cf (energy of  $-31.1$  a.u.; Fe–Cu distance of  $12.7$  Å) (**Fig. 6B**); and (iii) an intermediate configuration, which includes the hydrophobic patches and some residues of the electrostatic patches (energy of  $-30.1$  a.u.; Fe–Cu distance of  $12.2$  Å) (**Fig. 6C**). The fact that Pc is not present in many diatom species suggests that its heterologous acquisition may be relatively recent, and therefore, the [Cf:Pc] complex in *T. oceanica* would not have yet achieved a prevalent configuration optimized for ET.

Surprisingly, the clearly more favorable energies (energy of  $-38$  to  $-36$  a.u.) correspond to a cluster of very similar orientations, in which the electrostatic patches of both proteins establish strong interactions, also involving the additional positive groups outside the usual region of ET in Cf. However, in these orientations, the Cu and the Fe are located at a long distance

from each other (Fe–Cu distance of  $\approx 20$  Å) (**Fig. 6D**, **Supplementary Fig. S1**). Obviously, these orientations also show a long distance from the Fe in Cf to the groups that form the hydrophobic patch of Pc, and in particular to the Cu-binding H87 residue (H88 in the sequence of *T. oceanica* Pc) (**Fig. 6D**). The imidazole of H87 defines the shortest path from the copper atom to the protein surface ( $\approx 6$  Å) and forms the ET pathway in Pc from Cf and to PSI in cyanobacteria, green algae and plants (**Fig. 5A**), as clearly demonstrated by kinetic and structural data (Ubbink et al. 1998, Hippler and Drepper 2006, Caspy et al. 2020). However, in the apparently unproductive orientations of lowest energy in *T. oceanica*, the highly conserved Y84 residue in Pc (typically referred to as Y83 in cyanobacterial and eukaryotic Pc) points directly toward the heme-binding Y1 of Cf (Y1–Y84 distance of  $5.1$  Å; Fe–Y84 distance of  $9.9$  Å) (**Fig. 6D**). Based on the reactivity of Pc with inorganic complexes, as well as on theoretical studies, it was previously proposed that Y83 could act as another potential ET pathway in Pc (reviewed in Redinbo et al. 1994). However, this hypothesis was later discarded in the interaction of Pc with Cf and PSI (Ubbink et al. 1998, Hippler and Drepper 2006, Caspy et al. 2020). Therefore, it could be a matter of discussion whether this alternative ET pathway involving Y83—not active in green Pcs—is active or not in the heterologously acquired diatom Pc.

### Final Remarks

One of the most fascinating facts in the evolution of the ET from Cb<sub>6</sub>f to PSI is that while the overall backbone structures of the involved proteins are well conserved from prokaryotic to eukaryotic organisms, there are however significant differences, mainly affecting the electrostatic surface potential, which imply the appearance of functional areas with their own distinctive characteristics in the different types of photosynthetic organisms.

The green and red lineages comprise the two main lines in the evolution of eukaryotic photosynthetic organisms from a common ancestor. This ancestral organism resulted from an endosymbiotic event, in which a cyanobacterium ancestor gave origin to the eukaryotic chloroplast. Thus, in both the green- and red-type chloroplasts, the exit point is cyanobacterial photosynthesis, in which a shorter Psaf protein does not play a crucial role in the binding of the two soluble alternative electron donors, Pc and Cc<sub>6</sub>. Moreover, in cyanobacteria, the two soluble carriers do not have electrostatic characteristics widely shared among these organisms, predominating proteins of either almost neutral or strongly positive character, that have a complementary counterpart on the surface of the Cf partners.

In eukaryotic organisms, the evolution of the ET from Cb<sub>6</sub>f to PSI has developed conserved negative electrostatic patches in the soluble carriers, parallel to positive complementary areas of interaction in the two membrane complexes (in Cf and Psaf-PSI). However, within this general framework, the green line has developed areas of interaction with a stronger electrostatic charge, with a higher affinity between partners and a more

efficient ET, at the cost of limiting the turnover of the complexes. On the other hand, the red line seems to have developed areas of interaction with a weaker electrostatic charge, with a lower affinity between partners and a less efficient ET, favoring instead the exchange of proteins, and thus increasing the turnover of the process (Fig. 2B). However, and as a final conclusion, although following different strategies, the overall efficiency of the ET process from Cb<sub>6</sub>f to PSI is similar in the two main branches of eukaryotic photosynthesis, which represents an interesting example of molecular evolution in which proteins have optimized their function using different ways.

## Supplementary Data

Supplementary data are available at PCP online.

## Funding

The Spanish Ministry of Economy, Industry and Competitiveness (BIO2015-64169-P and BIO2016-79930-R) and the Andalusian Government (PAIDI BIO-022). These grants were partially financed by the EU FEDER Program. C.C. is the recipient of a FPU Program fellowship (FPU16/04040; Spanish Ministry of Education, Culture and Sports). We acknowledge the support of the publication fee by the CSIC Open Access Publication Support Initiative through its Unit of Information Resources for Research (URICI).

## Conflict of Interest

On behalf of all authors, the corresponding author states that there is no conflict of interest.

## References

- Abagyan, R., Lee, W.H., Raush, E., Budagyan, L., Totrov, M., Sundstrom, M., et al. (2006) Disseminating structural genomics data to the public: from a data dump to an animated story. *Trends Biochem. Sci.* 31: 76–78.
- Akazaki, H., Kawai, F., Hosokawa, M., Hama, T., Chida, H., Hirano, T., et al. (2009) Crystallization and structural analysis of cytochrome *c*<sub>6</sub> from the diatom *Phaeodactylum tricornutum* at 1.5 Å resolution. *Biosci. Biotechnol. Biochem.* 73: 189–191.
- Antoshvili, M., Caspy, I., Hippler, M. and Nelson, N. (2019) Structure and function of photosystem I in *Cyanidioschyzon merolae*. *Photosynth. Res.* 139: 499–508.
- Bendall, D.S. and Howe, C.J. (2016) The interaction between cytochrome *f* and plastocyanin or cytochrome *c*<sub>6</sub>. In *Cytochrome Complexes: Evolution, Structures, Energy Transduction, and Signaling. Advances in Photosynthesis and Respiration* 41. Edited by Cramer, W.A. and Kallas, T. pp. 631–655. Springer, Dordrecht.
- Bernal-Bayard, P., Molina-Heredia, F.P., Hervás, M. and Navarro, J.A. (2013) Photosystem I reduction in diatoms: as complex as the green lineage systems but less efficient. *Biochemistry* 52: 8687–8695.
- Bernal-Bayard, P., Pallara, C., Castell, C., Molina-Heredia, F.P., Fernández-Recio, J., Hervás, M., et al. (2015) Interaction of photosystem I from *Phaeodactylum tricornutum* with plastocyanins as compared with its native cytochrome *c*<sub>6</sub>: reunion with a lost donor. *Biochim. Biophys. Acta* 1847: 1549–1559.
- Blaby-Haas, C.E. and Merchant, S.S. (2012) The ins and outs of algal metal transport. *Biochim. Biophys. Acta* 1823: 1531–1552.
- Blankenship, R.E. (2014) *Molecular Mechanisms of Photosynthesis*, 2nd edn. Wiley-Blackwell, Chichester, UK.
- Bottin, H. and Mathis, P. (1985) Interaction of plastocyanin with the photosystem I reaction center: a kinetic study by flash absorption spectroscopy. *Biochemistry* 24: 6453–6460.
- Bowler, C., Vardi, A. and Allen, A.E. (2010) Oceanographic and biogeochemical insights from diatom genomes. *Ann. Rev. Mar. Sci.* 2: 333–365.
- Busch, A. and Hippler, M. (2011) The structure and function of eukaryotic photosystem I. *Biochim. Biophys. Acta* 1807: 864–877.
- Canutescu, A.A., Shelenkov, A.A. and Dunbrack, R.L. (2003) A graph-theory algorithm for rapid protein side-chain prediction. *Protein Sci.* 12: 2001–2014.
- Case, D.A. (2019) *Amber 2019*, University of California, San Francisco.
- Caspy, I., Borovikova-Sheinker, A., Klaiman, D., Shkolnisky, Y. and Nelson, N. (2020) The structure of a triple complex of plant photosystem I with ferredoxin and plastocyanin. *Nat. Plants* 6: 1300–1305.
- Castell, C., Bernal-Bayard, P., Ortega, J.M., Roncel, M., Hervás, M. and Navarro, J.A. (2021) The heterologous expression of a plastocyanin in the diatom *Phaeodactylum tricornutum* improves cell growth under iron-deficient conditions. *Physiol. Plant.* 171: 277–290.
- Cheatham, T.E., Cieplak, P. and Kollman, P.A. (1999) A modified version of the Cornell et al. force field with improved sugar pucker phases and helical repeat. *J. Biomol. Struct. Dyn.* 16: 845–862.
- Cheng, T.M., Blundell, T.L. and Fernandez-Recio, J. (2007) pyDock: electrostatics and desolvation for effective scoring of rigid-body protein-protein docking. *Proteins* 68: 503–515.
- Chi, Y.-I., Huang, L.-S., Zhang, Z., Fernández-Velasco, J.G. and Berry, E.A. (2000) X-ray structure of a truncated form of cytochrome *f* from *Chlamydomonas reinhardtii*. *Biochemistry* 39: 7689–7701.
- Cramer, W.A. (2019) Structure–function of the cytochrome *b<sub>6</sub>f* lipoprotein complex: a scientific odyssey and personal perspective. *Photosynth. Res.* 139: 53–65.
- Crowley, P.B., Otting, G., Schlarb-Ridley, B.G., Canters, G.W. and Ubbink, M. (2001) Hydrophobic interactions in a cyanobacterial plastocyanin-cytochrome *f* complex. *J. Am. Chem. Soc.* 123: 10444–10453.
- Crowley, P.B., Vintonenko, N., Bullerjahn, G.S. and Ubbink, M. (2002) Plastocyanin-cytochrome *f* interactions: the influence of hydrophobic patch mutations studied by NMR spectroscopy. *Biochemistry* 41: 15698–15705.
- Cruz-Gallardo, I., Díaz-Moreno, I., Díaz-Quintana, A. and De la Rosa, M.A. (2012) The cytochrome *f*–plastocyanin complex as a model to study transient interactions between redox proteins. *FEBS Lett.* 586: 646–652.
- De la Rosa, M.A., Molina-Heredia, F.P., Hervás, M. and Navarro, J.A. (2006) Convergent evolution of cytochrome *c*<sub>6</sub> and plastocyanin. The evolutionary pathways of the two proteins are connected to the geochemical changes in iron and copper availabilities. In *Photosystem I: The Light Driven Plastocyanin:Ferredoxin Oxidoreductase. Advances in Photosynthesis and Respiration*, Vol. 24. Edited by Golbeck, J.H. pp. 683–696. Springer, Dordrecht, The Netherlands.
- Díaz-Moreno, I., Díaz-Quintana, A., Molina-Heredia, F.P., Nieto, P.M., Hansson, Ö., De la Rosa, M.A., et al. (2005) NMR analysis of the transient complex between membrane photosystem I and soluble cytochrome *c*<sub>6</sub>. *J. Biol. Chem.* 280: 7925–7931.
- Díaz-Moreno, I., Hulsker, R., Skubak, P., Foerster, J.M., Cavazzini, D., Finiguerra, M.G., et al. (2014) The dynamic complex of cytochrome *c*<sub>6</sub> and cytochrome *f* studied with paramagnetic NMR spectroscopy. *Biochim. Biophys. Acta* 1837: 1305–1315.
- Díaz-Quintana, A., Hervás, M., Navarro, J.A. and De la Rosa, M.A. (2008) Plastocyanin and cytochrome *c*<sub>6</sub>: the soluble electron carriers between the cytochrome *b<sub>6</sub>f* complex and photosystem I. In *Photosynthetic Protein Complexes: A Structural Approach*. Edited by Fromme, P. pp. 181–200. Wiley-VCH Verlag GmbH & Co. KGaA, Weinheim.

- Drepper, F., Hippler, M., Nitschke, W. and Haehnel, W. (1996) Binding dynamics and electron transfer between plastocyanin and photosystem I. *Biochemistry* 35: 1282–1295.
- Falkowski, P.G., Katz, M.E., Knoll, A.H., Quigg, A., Raven, J.A., Schofield, O., et al. (2004) The evolution of modern eukaryotic phytoplankton. *Science* 305: 354–360.
- Farah, J., Rappaport, F., Choquet, Y., Joliot, P. and Rochaix, J.-D. (1995) Isolation of a *psaF* deficient mutant of *Chlamydomonas reinhardtii*: efficient interaction of plastocyanin with the photosystem I reaction center is mediated by the *PsaF* subunit. *EMBO J.* 14: 4976–4984.
- Fedorov, V.A., Kovalenko, I.B., Khrushev, S.S., Ustinin, D.M., Antal, T.K., Riznichenko, G.Y., et al. (2019) Comparative analysis of plastocyanin-cytochrome *f* complex formation in higher plants, green algae and cyanobacteria. *Physiol. Plant.* 166: 320–335.
- Field, C.B., Behrenfeld, M.J., Randerson, J.T. and Falkowski, P. (1998) Primary production of the biosphere: integrating terrestrial and oceanic components. *Science* 281: 237–240.
- Finazzi, G., Sommer, F. and Hippler, M. (2005) Release of oxidized plastocyanin from photosystem I limits electron transfer between photosystem I and cytochrome *b<sub>6</sub>f* complex *in vivo*. *Proc. Natl. Acad. Sci. USA* 102: 7031–7036.
- Frazão, C., Soares, C.M., Carrondo, M.A., Pohl, E., Dauter, Z., Wilson, K.S., et al. (1995) *Ab initio* determination of the crystal structure of cytochrome *c<sub>6</sub>* and comparison with plastocyanin. *Structure* 3: 1159–1169.
- Gabb, H.A., Jackson, R.M. and Sternberg, M.J. (1997) Modelling protein docking using shape complementarity, electrostatics and biochemical information. *J. Mol. Biol.* 272: 106–120.
- García-Cañas, R., Giner-Lamia, J., Florencio, F.J. and López-Maury, L. (2021) López-Maury L (2021) A protease-mediated mechanism regulates the cytochrome *c<sub>6</sub>*/plastocyanin switch in *Synechocystis* sp. PCC 6803. *Proc. Natl. Acad. Sci. USA* 118: e2017898118.
- Giammona, D.A. (1984) *An examination of conformational flexibility in porphyrins and bulky-ligand binding in myoglobin*. Ph.D. Thesis. University of California, Davis.
- Gong, X.-S., Wen, J.Q., Fisher, N.E., Young, S., Howe, C.J., Bendall, D.S., et al. (2000) The role of individual lysine residues in the basic patch on turnip cytochrome *f* for electrostatic interactions with plastocyanin *in vitro*. *Eur. J. Biochem.* 267: 3461–3468.
- Gross, E.L. and Pearson, D.C. (2003) Brownian dynamics simulations of the interaction of *Chlamydomonas* cytochrome *f* with plastocyanin and cytochrome *c<sub>6</sub>*. *Biophys. J.* 85: 2055–2068.
- Groussman, R.D., Parker, M.S. and Armbrust, E.V. (2015) Diversity and evolutionary history of iron metabolism genes in diatoms. *PLoS One* 10: e0129081.
- Grove, T.Z. and Kostic, N.M. (2003) Metalloprotein association, self-association, and dynamics governed by hydrophobic interactions: simultaneous occurrence of gated and true electron-transfer reactions between cytochrome *f* and cytochrome *c<sub>6</sub>* from *Chlamydomonas reinhardtii*. *J. Am. Chem. Soc.* 125: 10598–10607.
- Guo, J., Annett, A.L., Taylor, R.L., Lapi, S., Ruth, T.J. and Maldonado, M.T. (2010) Copper-uptake kinetics of coastal and oceanic diatoms. *J. Phycol.* 46: 1218–1228.
- Guo, J., Green, B.R. and Maldonado, M.T. (2015) Sequence analysis and gene expression of potential components of copper transport and homeostasis in *Thalassiosira pseudonana*. *Protist* 166: 58–77.
- Guss, J.M. and Freeman, H.C. (1983) Structure of oxidized poplar plastocyanin at 1.6 Å resolution. *J. Mol. Biol.* 169: 521–563.
- Haddadian, E.J. and Gross, E.L. (2005) Brownian dynamics study of cytochrome *f* interactions with cytochrome *c<sub>6</sub>* and plastocyanin in *Chlamydomonas reinhardtii* plastocyanin, and cytochrome *c<sub>6</sub>* mutants. *Biophys. J.* 88: 2323–2339.
- Haddadian, E.J. and Gross, E.L. (2006) A brownian dynamics study of the effects of cytochrome *f* structure and deletion of its small domain in interactions with cytochrome *c<sub>6</sub>* and plastocyanin in *Chlamydomonas reinhardtii*. *Biophys. J.* 90: 566–577.
- Haehnel, W., Jansen, T., Gause, K., Klossgen, R.B., Stahl, B., Michl, D., et al. (1994) Electron transfer from plastocyanin to photosystem I. *EMBO J.* 13: 1028–1038.
- Hall, D.O. (1976) Photobiological energy conversion. *FEBS Lett.* 64: 6–16.
- Hervás, M., Navarro, J.A. and De la Rosa, M.A. (2003) Electron transfer between soluble proteins and membrane complexes in photosynthesis. *Acc. Chem. Res.* 36: 798–805.
- Hervás, M., Navarro, J.A., Díaz, A., Bottin, H. and De la Rosa, M.A. (1995) Laser-flash kinetic analysis of the fast electron transfer from plastocyanin and cytochrome *c<sub>6</sub>* to photosystem I. Experimental evidence on the evolution of the reaction mechanism. *Biochemistry* 34: 11321–11326.
- Hippler, M. and Drepper, F. (2006) Electron transfer between photosystem I and plastocyanin or cytochrome *c<sub>6</sub>*. In *Photosystem I: The Light Driven Plastocyanin:Ferredoxin Oxidoreductase. Advances in Photosynthesis and Respiration*, Vol. 24. Edited by Golbeck, J.H. pp. 499–513. Springer, Dordrecht, The Netherlands.
- Hippler, M., Drepper, F., Haehnel, W. and Rochaix, J.D. (1998) The N-terminal domain of *PsaF*: precise recognition site for binding and fast electron transfer from cytochrome *c<sub>6</sub>* and plastocyanin to photosystem I of *Chlamydomonas reinhardtii*. *Proc. Natl. Acad. Sci. USA* 95: 7339–7344.
- Hippler, M., Reichert, J., Sutter, M., Zak, E., Altschmied, L., Schröer, U., et al. (1996) The plastocyanin binding domain of photosystem I. *EMBO J.* 15: 6374–6384.
- Hippmann, A.A., Schuback, N., Moon, K.M., McCrow, J.P., Allen, A.E., Foster, L.J., et al. (2017) Contrasting effects of copper limitation on the photosynthetic apparatus in two strains of the open ocean diatom *Thalassiosira oceanica*. *PLoS One* 12: e0181753.
- Ho, T.Y., Quigg, A., Finkel, Z.V., Milligan, A.J., Wyman, K., Falkowski, P.G., et al. (2003) The elemental composition of some marine phytoplankton. *J. Phycol.* 39: 1145–1159.
- Inoue, T., Sugawara, H., Hamanaka, S., Tsukui, H., Suzuki, E., Kohzuma, T., et al. (1999) Crystal structure determinations of oxidized and reduced plastocyanin from the cyanobacterium *Synechococcus* sp. PCC 7942. *Biochemistry* 38: 6063–6069.
- Jiménez-García, B., Pons, C. and Fernández-Recio, J. (2013) pyDockWEB: a web server for rigid-body protein-protein docking using electrostatics and desolvation scoring. *Bioinformatics* 29: 1698–1699.
- Kannt, A., Young, S. and Bendall, D.S. (1996) The role of acidic residues of plastocyanin in its interaction with cytochrome *f*. *Biochim. Biophys. Acta* 1277: 115–126.
- Klughammer, C. and Schreiber, U. (2016) Deconvolution of ferredoxin, plastocyanin, and P700 transmittance changes in intact leaves with a new type of kinetic LED array spectrophotometer. *Photosynth. Res.* 128: 195–214.
- Kohzuma, T., Inoue, T., Yoshizaki, F., Sasakawa, Y., Onodera, K., Nagatomo, S., et al. (1999) The structure and unusual pH dependence of plastocyanin from the fern *Dryopteris crassirhizoma*. The protonation of an active site histidine is hindered by  $\pi$ - $\pi$  interactions. *J. Biol. Chem.* 274: 11817–11823.
- Kong, L. and Price, N.M. (2019) Functional CTR-type Cu(I) transporters in an oceanic diatom. *Environ. Microbiol.* 21: 98–110.
- Kong, L. and Price, N.M. (2020) Identification of copper-regulated proteins in an oceanic diatom, *Thalassiosira oceanica* 1005. *Metallomics* 12: 1106–1117.
- Kuhlgert, S., Drepper, F., Fufezan, C., Sommer, F. and Hippler, M. (2012) Residues *PsaB* Asp612 and *PsaB* Glu613 of photosystem I confer pH-dependent binding of plastocyanin and cytochrome *c<sub>6</sub>*. *Biochemistry* 51: 7297–7303.
- Kurusu, G., Zhang, H., Smith, J.L. and Cramer, W.A. (2003) Structure of the cytochrome *b<sub>6</sub>f* complex of oxygenic photosynthesis: tuning the cavity. *Science* 302: 1009–1014.
- Lange, C., Cornvik, T., Díaz-Moreno, I. and Ubbink, M. (2005) The transient complex of poplar plastocyanin with cytochrome *f*: effects of ionic strength and pH. *Biochim. Biophys. Acta* 1707: 179–188.



- Levy, J.L., Angel, B.M., Stauber, J.L., Poon, W.L., Simpson, S.L., Cheng, S.H., et al. (2008) Uptake and internalisation of copper by three marine microalgae: Comparison of copper-sensitive and copper-tolerant species. *Aquat. Toxicol.* 89: 82–93.
- Lommer, M., Specht, M., Roy, A.S., Kraemer, L., Andreson, R., Gutowska, M. A., et al. (2012) Genome and low-iron response of an oceanic diatom adapted to chronic iron limitation. *Genome Biol.* 13: R661–20.
- Marchetti, A., Schruth, D.M., Durkin, C.A., Parker, M.S., Kodner, R.B., Berthiaume, C.T., et al. (2012) Comparative metatranscriptomics identifies molecular bases for the physiological responses of phytoplankton to varying iron availability. *Proc. Natl. Acad. Sci. USA* 109: E317–E325.
- Martinez, S.E., Huang, D., Szczepaniak, A., Cramer, W.A. and Smith, J.L. (1994) Crystal structure of the chloroplast cytochrome *f* reveals a novel cytochrome fold and unexpected heme ligation. *Structure* 2: 95–105.
- Merchant, S., Schmollinger, S., Strenkert, D., Moseley, J. and Blaby-Haas, C.E. (2020) From economy to luxury: copper homeostasis in *Chlamydomonas* and other algae. *Biochim. Biophys. Acta Mol. Cell Res.* 1867: 118822.
- Meyer, T.E., Zhao, Z.G., Cusanovich, M.A. and Tollin, G. (1993) Transient kinetics of electron transfer from a variety of c-type cytochromes to plastocyanin. *Biochemistry* 32: 4552–4559.
- Molina-Heredia, F.P., Wastl, J., Navarro, J.A., Bendall, D.S., Hervás, M., Howe, C.J., et al. (2003) A new function for an old cytochrome? *Nature* 424: 33–34.
- Moore, J.K. and Braucher, O. (2008) Sedimentary and mineral dust sources of dissolved iron to the world ocean. *Biogeosciences* 5: 631–656.
- Musiani, F., Dikiy, A., Semenov, A.Y. and Ciurli, S. (2005) Structure of the intermolecular complex between plastocyanin and cytochrome *f* from spinach. *J. Biol. Chem.* 280: 18833–18841.
- Navarro, J.A., Hervás, M. and De la Rosa, M.A. (2011) Purification of plastocyanin and cytochrome *c<sub>6</sub>* from plants, green algae and cyanobacteria. In *Photosynthesis Research Protocols, Methods in Molecular Biology*, Vol. 684. Edited by Carpentier, R. pp. 79–94.
- Navarro, J.A., Lowe, C.E., Amons, R., Kohzuma, T., Canters, G.W., De la Rosa, M.A., et al. (2004) Functional characterization of the evolutionarily divergent fern plastocyanin. *Eur. J. Biochem.* 271: 3449–3456.
- Nosenko, T., Lidie, K.L., Van Dolah, F.M., Lindquist, E., Cheng, J.F. and Bhattacharya, D. (2006) Chimeric plastid proteome in the florida “red tide” dinoflagellate *Karenia brevis*. *Mol. Biol. Evol.* 23: 2026–2038.
- Nouet, C., Motte, P. and Hanikenne, M. (2011) Chloroplastic and mitochondrial metal homeostasis. *Trends Plant Sci.* 16: 395–404.
- Peers, G. and Price, N.M. (2006) Copper-containing plastocyanin used for electron transport by an oceanic diatom. *Nature* 441: 341–344.
- Pettersen, E.F., Goddard, T.D., Huang, C.C., Couch, G.S., Greenblatt, D.M., Meng, E.C. and Ferrin, T.E. (2004) UCSF Chimera—a visualization system for exploratory research and analysis. *J. Comput. Chem.* 25: 1605–1612.
- Pierella Karlusich, J.J., Lodeyro, A.F. and Carrillo, N. (2014) The long goodbye: the rise and fall of flavodoxin during plant evolution. *J. Exp. Bot.* 65: 5161–5178.
- Qin, L. and Kostic, N.M. (1993) Importance of protein rearrangement in the electron-transfer reaction between the physiological partners cytochrome *f* and plastocyanin. *Biochemistry* 32: 6073–6080.
- Redinbo, M.R., Yeates, T.O. and Merchant, S. (1994) Plastocyanin: structural and functional analysis. *J. Bioenerg. Biomembr.* 26: 49–66.
- Rizkallah, M.R., Frickenhaus, S., Trimborn, S., Harms, L., Moustafa, A., Benes, V., et al. (2020) Deciphering patterns of adaptation and acclimation in the transcriptome of *Phaeocystis antarctica* to changing iron conditions. *J. Phycol.* 56: 747–760.
- Roncel, M., González-Rodríguez, A.A., Naranjo, B., Bernal-Bayard, P., Lindahl, A.M., Hervás, M., et al. (2016) Iron deficiency induces a partial inhibition of the photosynthetic electron transport and a high sensitivity to light in the diatom *Phaeodactylum tricornutum*. *Front. Plant Sci.* 7: 1–14.
- Šali, A. and Blundell, T.L. (1993) Comparative protein modelling by satisfaction of spatial restraints. *J. Mol. Biol.* 234: 779–815.
- Sancho, J. (2006) Flavodoxins: sequence, folding, binding, function and beyond. *Cell. Mol. Life Sci.* 63: 855–864.
- Schilder, J. and Ubbink, M. (2013) Formation of transient protein complexes. *Curr. Opin. Struct. Biol.* 23: 911–918.
- Schlarb-Ridley, B.G., Bendall, D.S. and Howe, C.J. (2003) Relation between interface properties and kinetics of electron transfer in the interaction of cytochrome *f* and plastocyanin from plants and the cyanobacterium *Phormidium laminosum*. *Biochemistry* 42: 4057–4063.
- Sétif, P. (2006) Electron transfer from the bound iron-sulfur clusters to ferredoxin/flavodoxin: kinetic and structural properties of ferredoxin/flavodoxin reduction by photosystem I. In *Photosystem I: The Light Driven Plastocyanin:Ferredoxin Oxidoreductase. Advances in Photosynthesis and Respiration*, Vol. 24. Edited by Golbeck, J.H. pp. 439–454. Springer, Dordrecht, The Netherlands.
- Shahrokh, S., Orendt, A., Yost, G.S. and Cheatham, T.E. III (2012) Quantum mechanically derived AMBER-compatible heme parameters for various states of the cytochrome P450 catalytic cycle. *J. Comput. Chem.* 33: 119–133.
- Shen, M.Y. and Šali, A. (2006) Statistical potential for assessment and prediction of protein structures. *Protein Sci.* 15: 2507–2524.
- Sigfridsson, K., He, S., Modi, S., Bendall, D.S., Gray, J. and Hansson, Ö. (1996) A comparative flash-photolysis study of electron transfer from pea and spinach plastocyanins to spinach photosystem I. A reaction involving a rate-limiting conformational change. *Photosynth. Res.* 50: 11–21.
- Sommer, F., Drepper, F., Haehnel, W. and Hippler, M. (2004) The hydrophobic recognition site formed by residues PsaA-Trp651 and PsaB-Trp627 of photosystem I in *Chlamydomonas reinhardtii* confers distinct selectivity for binding of plastocyanin and cytochrome *c<sub>6</sub>*. *J. Biol. Chem.* 279: 20009–20017.
- Sommer, F., Drepper, F., Haehnel, W. and Hippler, M. (2006) Identification of precise electrostatic recognition sites between cytochrome *c<sub>6</sub>* and the photosystem I subunit PsaF using mass spectrometry. *J. Biol. Chem.* 281: 35097–35103.
- Soriano, G.M., Cramer, W.A. and Krishtalik, L.I. (1997) Electrostatic effects on electron-transfer kinetics in the cytochrome *f* plastocyanin complex. *Biophys. J.* 73: 3265–3276.
- Stroebel, D., Choquet, Y., Popot, J.-L. and Picot, D. (2003) An atypical heme in the cytochrome *b<sub>6</sub>f* complex. *Nature* 426: 413–418.
- Theune, M.L., Hildebrandt, S., Steffen-Heins, A., Bilger, W., Gutekunst, K. and Appel, J. (2021) In-vivo quantification of electron flow through photosystem I—cyclic electron transport makes up about 35% in a cyanobacterium. *Biochim. Biophys. Acta Bioenerg.* 1862: 148353.
- Twining, B.S.B. and Baines, S.B. (2013) The trace metal composition of marine phytoplankton. *Ann. Rev. Mar. Sci.* 5: 191–215.
- Ubbink, M., Ejdebäck, M., Karlsson, B.G. and Bendall, D.S. (1998) The structure of the complex of plastocyanin and cytochrome *f*, determined by paramagnetic NMR and restrained rigid-body molecular dynamics. *Structure* 6: 323–335.
- Yamada, S., Park, S.Y., Shimizu, H., Koshizuka, Y., Kadokura, K., Satoh, T., et al. (2000) Structure of cytochrome *c<sub>6</sub>* from the red alga *Porphyra yezoensis* at 1.57 Å resolution. *Acta Crystallogr. D: Biol. Crystallogr.* 56: 1577–1582.